

Spin-induced optical second harmonic generation in the centrosymmetric magnetic semiconductors EuTe and EuSe

B. Kaminski¹, M. Lafrentz¹, R. V. Pisarev², D. R. Yakovlev^{1,2}, V. V. Pavlov², V. A. Lukoshkin²,
A. B. Henriques³, G. Springholz⁴, G. Bauer⁴, E. Abramof⁵, P. H. O. Rappl⁵, and M. Bayer¹

¹*Experimentelle Physik 2, Technische Universität Dortmund, D-44221 Dortmund, Germany*

²*Ioffe Physical-Technical Institute, Russian Academy of Sciences, 194021 St. Petersburg, Russia*

³*Instituto de Física, Universidade de São Paulo, 05315-970 São Paulo, Brazil*

⁴*Institut für Halbleiter- und Festkörperphysik, Johannes Kepler Universität Linz, 4040 Linz, Austria and*

⁵*LAS-INPE, 12227-010 São José dos Campos, Brazil*

(Dated: May 29, 2018)

Spectroscopy of the centrosymmetric magnetic semiconductors EuTe and EuSe reveals spin-induced optical second harmonic generation (SHG) in the band gap vicinity at 2.1-2.4 eV. The magnetic field and temperature dependence demonstrates that the SHG arises from the bulk of the materials due to a novel type of nonlinear optical susceptibility caused by the magnetic dipole contribution combined with spontaneous or induced magnetization. This spin-induced susceptibility opens access to a wide class of centrosymmetric systems by harmonics generation spectroscopy.

PACS numbers: 75.50.Pp, 42.65.Ky, 78.20.Ls

Nonlinear optics is a highly active field of basic and applied research with optical harmonics generation playing a particularly important role [1, 2]. Harmonics generation is associated with higher order optical susceptibilities, and opens access to unique information about the crystallographic, electronic and magnetic structure of solids that is inaccessible by linear optics [1, 2, 3]. Second harmonic generation (SHG) has attracted most interest, because of its exceptional sensitivity to space and time symmetry violations [3] and its importance for technological applications. Spectroscopy of semiconductors using SHG has been, however, mostly limited to narrow spectral ranges [4, 5]. Recently, SHG was studied in detail for the *noncentrosymmetric* semiconductors GaAs, CdTe and (Cd,Mn)Te [6, 7], where SHG is allowed in electric-dipole (ED) approximation. Two mechanisms of magnetic-field-induced SHG have been disclosed, based on changing ED contributions by mixing with magnetically-induced terms. In *centrosymmetric* materials with inversion symmetry SHG is forbidden in ED approximation, which imposes severe restrictions on the crystalline solids and artificial structures that can be explored by SHG.

This restriction can be overcome by processes based on magnetic-dipole (MD) or electric-quadrupole (EQ) nonlinear susceptibilities. Other opportunities may be opened up by external or internal perturbations that break either space-inversion or time-reversal symmetry. For example, an applied electric field breaks the space-inversion symmetry in centrosymmetric materials so that ED-SHG becomes allowed [8]. It would be highly attractive to find the counterpart SHG related exclusively to MD contributions triggered by applied magnetic fields or magnetic ordering. Evidently, the search for such mechanisms is facilitated in centrosymmetric materials, where crystallographic ED and EQ contributions to SHG vanish.

In this Letter we report on spin-induced SHG in

the centrosymmetric magnetic semiconductors EuTe and EuSe. No SHG was detected in the antiferromagnetic and paramagnetic phases. However, when a magnetic field is applied, SHG arises due to breaking of the antiferromagnetic order or by polarization of the paramagnetic phase, both resulting in appearance of a net magnetization. The observed spin-related nonlinearities arise due to a novel type of nonlinear optical susceptibility caused by the MD contribution in combination with spontaneous or induced magnetization.

Europium chalcogenides EuX ($X=O, S, Se, \text{ and } Te$) are magnetic semiconductors crystallizing in the centrosymmetric cubic rock salt structure $m3m$. They possess unique physical properties determined by the electronic structure in which the strongly localized $4f^7$ electrons of Eu^{2+} ions with spin $S = 7/2$ are involved [9]. EuX are classical Heisenberg magnets where the competition between nearest and next-nearest neighbor exchange integrals results in magnetic phase diagrams that can include antiferro- (AFM), ferri- (FIM), and ferromagnetic (FM) ordering as well as a paramagnetic phase at elevated temperatures [9, 10]. EuTe is antiferromagnetic with a Néel temperature $T_N=9.6$ K and a critical field $B_c = 7.2$ T above which it becomes ferromagnetically saturated. EuSe is metamagnetic with $T_N = 4.6$ K and shows a mixed AFM and FIM ordering below 2.8 K. At $T < 2$ K and in a magnetic field above a critical value of 0.2 T EuSe is in the FM phase [10]. EuX exhibit strong linear magneto-optical effects [11, 12, 13], due to what they attract interest for potential applications in spin injection and magneto-optical devices [14, 15, 16, 17, 18]. Nonlinear optical properties of these materials have not yet been explored.

The experimental technique is described in Ref. [6]. SHG spectra were recorded in transmission geometry using 8 ns pulses with a 10 Hz repetition rate generated by an optical parametric oscillator. Experiments were performed on EuTe and EuSe layers grown by molecular-

beam epitaxy on (111)-oriented BaF₂ substrates [12, 19]. The 1 μm thick layers were capped with a 40-nm-thick BaF₂ protective layer and the high sample quality was confirmed by x-ray analysis. The sample temperature was varied from 1.4 to 50 K. Magnetic fields up to $B=10$ T were applied in the Voigt geometry.

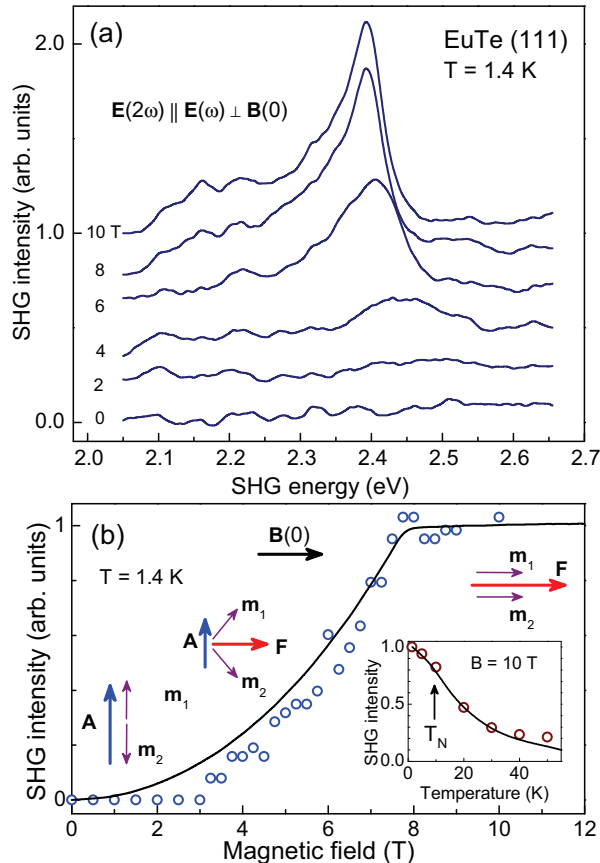


FIG. 1: (Color online) (a) SHG spectra of EuTe in different magnetic fields. Spectra are offset by 0.2 relative to each other. (b) Integral SHG intensity as function of magnetic field. Solid line gives normalized magnetization $M^2(B)$ [20]. Inset shows temperature dependence of peak intensity at $B = 10$ T. Line gives normalized $M^2(T)$ after Ref. [20].

Figure 1(a) displays the SHG spectra of EuTe recorded at different magnetic fields. At zero field, no SHG signal was detected in a wide temperature range below and above T_N . However, SHG appears at finite B in the vicinity of the band gap and its structure with a maximum at 2.4 eV and a shoulder at 2.2 eV is in good agreement with EuTe absorption spectra [12, 13]. As shown in Fig. 1(b), the integrated SHG intensity increases with field and saturates for $B > 7.5$ T. Remarkably, it follows the square magnetization of EuTe represented by the solid line, which saturates above $B_c=7.2$ T where all spins are collinearly aligned [20]. As is indicated by the arrows in Fig. 1(b), this magnetization stems from a

continuous transformation of the AFM ordering at $B=0$ to the FM one above B_c . At a fixed magnetic field of $B=10$ T, the SHG signal continuously decreases with increasing temperature and vanishes at about 50 K. As demonstrated by the insert of Fig. 1(b) this decrease follows approximately the $M^2(T)$ dependence [20]. Above T_N the SHG signal is obviously related to the paramagnetic spin polarization.

It is evident from Fig. 1 that the SHG mechanism in EuTe is controlled by the spin polarization of Eu^{2+} induced by external magnetic fields. The experiments on EuSe confirm this conclusion despite its complicated magnetic phase diagram [10]. Figure 2(a) shows that in the vicinity of the optical band gap around 2.1-2.4 eV, again a clear SHG signal appears at finite B , which is absent at $B=0$. The magnetic field dependence of the corresponding SHG intensity is shown in Fig. 2(b) for two experimental geometries with $\mathbf{E}(2\omega)\perp\mathbf{E}(\omega)$ and $\mathbf{E}(2\omega)\parallel\mathbf{E}(\omega)$. In both cases, the SHG intensity increases in a stepwise manner with increasing field, and shows two saturation regions, one between 0.01 and 0.2 T and a second one above 0.2 T. These steps are in good agreement with the critical fields for the magnetic phase transitions of EuSe [10]. It gives us a clear proof that the measured SHG arises from the bulk of the sample and not from the surface [21], because critical fields at the surface, and in particular in antiferromagnets, radically differ from those in bulk.

Two contributions to the nonlinear optical polarization can be expected in the EuX magnetic semiconductors. The one related to the crystallographic magnetic dipole (CMD) is [22]

$$P_i^{CMD}(2\omega) = i\varepsilon_0\chi_{ijk}^{(2)}E_j(\omega)B_k(\omega), \quad (1)$$

where $E_j(\omega)$ and $B_k(\omega)$ are the electric and magnetic fields of the fundamental light wave, respectively. $\chi_{ijk}^{(2)}$ is an axial third-rank tensor allowed in any medium [23]. The same type of tensor describes the Faraday effect, if in Eq. (1) the light field $B_k(\omega)$ is replaced by an external magnetic field $B_k(0)$, and the polarization $P_i(\omega)$ is excited at the fundamental frequency. In view of the strong Faraday effect in EuX compounds achieving 10^6 deg/cm [11] a significant MD contribution to the SHG is expected [22]. In bulk EuX with point group $m3m$ the tensor $\chi_{ijk}^{(2)}$ has only one non-vanishing independent component $xyz(c3)=-xzy(c3)$ [23], which, however, does not lead to any SHG intensity $I(2\omega)\propto|\mathbf{P}^{CMD}(2\omega)|^2$ because of the alternating sign change for every axis permutation.

Layers of EuTe and EuSe grown on BaF₂ substrate are known to acquire a small mismatch between sample and substrate lattice constants resulting in a weak trigonal distortion along the [111]-axis. Evidently this causes a symmetry reduction of the thin EuTe and EuSe layers to the trigonal centrosymmetric point group $\bar{3}m$ in the proximity of the interface. The tensor $\chi_{ijk}^{(2)}$ in this point group has one independent component $xyz(6)$ [23] which

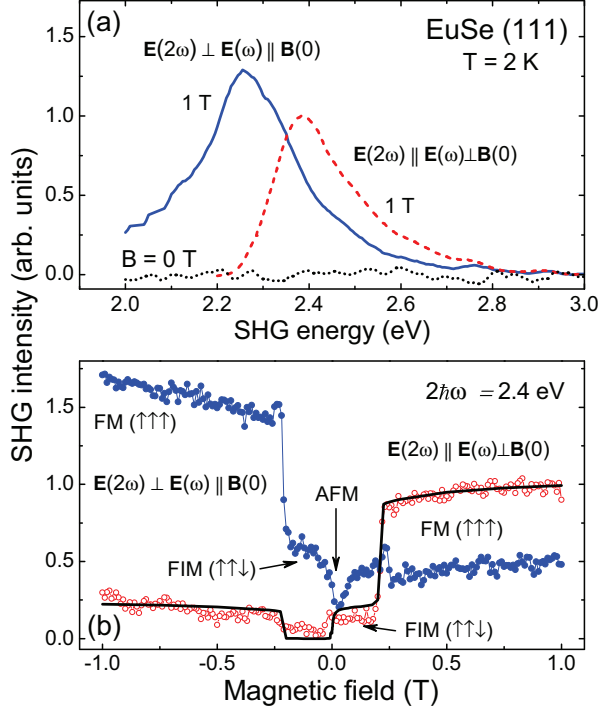


FIG. 2: (Color online) (a) Magnetic-field-induced SHG spectra in EuSe shown for zero field and for a saturation field of +1 T for two different measurement geometries. (b) SHG intensity vs magnetic field. The line gives normalized $[a + bM(B)]^2$ with $b/a = 4$ and $M(B)$ after Ref. [10].

may produce a small crystallographic MD contribution to the SHG signal.

A new type of nonlinear polarization can be induced if the parent crystal symmetry is broken by either magnetic field or magnetic ordering, both of which we introduce with the magnetic parameter $\mathbf{M}(0)$. The induced magnetic dipole (IMD) nonlinear polarization is

$$P_i^{IMD}(2\omega) = \varepsilon_0 \chi_{ijkl}^{(3)} E_j(\omega) B_k(\omega) M_l(0), \quad (2)$$

where $\chi_{ijkl}^{(3)}$ is a polar fourth-rank tensor [23].

In EuTe the magnetic ordering below T_N can be characterized by the magnetic moments \mathbf{m}_1 and \mathbf{m}_2 of the two sublattices with $|m_1| = |m_2|$. To describe the magnetic behavior of an antiferromagnet in external magnetic field we introduce a FM vector $\mathbf{F} = \mathbf{m}_1 + \mathbf{m}_2$ and an AFM vector $\mathbf{A} = \mathbf{m}_1 - \mathbf{m}_2$. The scheme in Fig. 1(b) shows the sublattice reorientation when the magnetic field is increased. Though \mathbf{F} and \mathbf{A} are composed of the same vectors \mathbf{m}_1 and \mathbf{m}_2 , their transformation properties are different. \mathbf{F} changes sign under time reversal, but not under space inversion, and thus transforms as a MD. The AFM vector \mathbf{A} does not induce any SHG signal, which qualitatively can be understood as follows: at $B=0$ \mathbf{m}_1 and \mathbf{m}_2 are oriented antiferromagnetically. Each mag-

netic sublattice induces a SHG signal via MD according to Eq. (2) with $\mathbf{M}(0) = \mathbf{m}_{1,2}$, but destructive interference from oppositely oriented sublattices annihilates the SHG signal since the relevant nonlinear polarization is an odd function of $\mathbf{M}(0)$. With increasing magnetic field the AFM ordering is transformed into a FM one and the destructive interference is continuously reduced. In this case $\mathbf{M}(0)$ in Eq. (2) should be associated with the ferromagnetic vector \mathbf{F} . The SHG signal increases with magnetic field and reaches saturation when the two sublattices become oriented ferromagnetically. Above T_N in the paramagnetic phase $\mathbf{M}(0) = \chi_p \mathbf{B}$, where χ_p is the paramagnetic susceptibility.

The rotational anisotropy of the SHG intensity detected for simultaneous rotation of linear polarizers for the fundamental and SHG light is a characteristic feature of the coherent SHG process giving an in-depth view on the symmetries involved. Corresponding diagrams for EuTe and EuSe are shown in Fig. 3 for the parallel $[\mathbf{E}(2\omega) \parallel \mathbf{E}(\omega)]$ and perpendicular $[\mathbf{E}(2\omega) \perp \mathbf{E}(\omega)]$ configuration. For EuTe the rotational anisotropies are twofold. In EuSe the rotational anisotropy is twofold in the parallel configuration but is transformed into a distorted fourfold anisotropy for the perpendicular case.

To model the rotational anisotropy of SHG intensity, the interference between IMD [Eq. (1)] and CMD [Eq. (2)] contributions should be taken into account

$$I(2\omega) \propto |\mathbf{P}^{IMD}|^2 + |\mathbf{P}^{CMD}|^2 \pm 2|\mathbf{P}^{IMD}\mathbf{P}^{CMD}|. \quad (3)$$

Here the signs \pm correspond to opposite orientations of $\mathbf{M}(0)$. The SHG intensities for the parallel and perpendicular configurations of fundamental and SHG light polarizations are

$$I_{\parallel}(2\omega) \propto \left[\pm \frac{F}{6} (\chi_{xxxx} + 5\chi_{xxyy} - \chi_{xyxy} - \chi_{yyxx}) \cos \varphi - \chi_{xyz} \cos 3(\alpha + \varphi) \right]^2, \quad (4)$$

$$I_{\perp}(2\omega) \propto \left[\pm \frac{F}{6} (\chi_{xxxx} - \chi_{xxyy} + 5\chi_{xyxy} - \chi_{yyxx}) \sin \varphi + \chi_{xyz} \sin 3(\alpha + \varphi) \right]^2, \quad (5)$$

where φ is the angle between the polarization plane of the fundamental light and the crystallographic $[11\bar{2}]$ axis and α is the sample azimuthal angle. As shown by Figs. 3(e) and 3(f), the IMD contribution calculated for the point group $m3m$ results in a twofold diagram, whereas the CMD contribution for the point group $3m$ results in a sixfold diagram. The modeling with the IMD contribution only, shown by solid lines in Figs. 3(a) and (d), are in satisfactory agreement for EuTe. For EuSe the parallel configuration is in qualitative agreement, but not the fourfold anisotropy in perpendicular configuration. The modeling with both contributions are shown by the shaded areas. Very good agreement is achieved for both EuTe and EuSe. The fitting procedure reveals a P^{IMD}/P^{CMD} ratio of $\sim 7/1$ for EuTe and $\sim 4/1$ for EuSe. Thus, the IMD contribution dominates over the CMD one, which allows us to conclude that the MD-SHG

process in EuX is mainly determined by the spin-induced mechanism. This is also confirmed by the vanishing SHG signal at elevated temperatures, shown in the insert of Fig. 1(b).

The negligible role of the CMD contribution for EuTe is confirmed by the fact that the magnetic field dependence of the SHG intensity $I(2\omega) \propto M^2$, as seen in Fig. 1(b). To account for the interference of CMD and IMD contributions in EuSe we compare in Fig. 2(b) $I(2\omega)$ with $[a + bM(B)]^2$ dependence taking $b/a=4$ similar to $P^{IMD}/P^{CMD}=4$ for the saturated magnetization. The observed asymmetry in the field dependence is well explained. Therefore, the observed SHG is due to the FM component of the spin system in EuX, which induces the MD contribution to SHG. The role of the external magnetic field is to induce the ferromagnetic component \mathbf{F} . SHG signals are observed also above T_N , when the

magnetic field polarizes the Eu^{2+} spins in a paramagnetic phase. Thus, application of the magnetic field to EuX leads to a new type of MD nonlinearity. It can be treated as a counterpart to electric field application to centrosymmetric media which breaks space inversion symmetry and allows ED-SHG processes.

The spin-induced nonlinearities in EuX can be analyzed in the framework of a microscopic model. For EuTe the valence band is formed by the $5p^6$ orbitals of Te^{2-} and the conduction band by the $5d$ and $6s$ orbitals of Eu^{2+} [9]. The $5d$ levels are split by the crystal field into t_{2g} and e_g subbands. The localized $4f^7$ states of Eu^{2+} are close to the top of the valence band. The optical band gap is determined by $4f^7 \rightarrow 5d(t_{2g})$ transitions. The SHG is explained taking into account nonlinearities involving an $^8S_{7/2}$ ground state and electronic levels within the conduction band, given by the $^7F_J Y$, where $J = 0, \dots, 6$ and Y is one of the three orbital states in the $5d(t_{2g})$ subset [13]. The main contributions to the spin-induced nonlinear susceptibility from each magnetic sublattice is

$$\frac{\langle ^8S_{7/2} | x | ^7F_J Y \rangle \langle ^7F_J Y | L_y | ^7F_{J'} Y' \rangle \langle ^7F_{J'} Y' | x | ^8S_{7/2} \rangle}{[E(^7F_{J'} Y') - \hbar\omega] [E(^7F_J Y) - 2\hbar\omega]}, \quad (6)$$

where L_y is the magnetic dipole operator and x is position of all seven electrons. It must be emphasized that only the magnetic dipole operator can couple the Y and Y' states, whereas their ED or EQ couplings are symmetry forbidden. Calculations, whose details will be given elsewhere, lead to vanishing of the spin-induced nonlinear susceptibility in the AFM phase, because the contributions from both magnetic sublattices cancel each other. The susceptibility increases when the Eu^{2+} spins are tilted towards the magnetic field. This explains the observed relation between the SHG intensity and the sample magnetization.

In conclusion, spin-induced SHG is found in the centrosymmetric magnetic semiconductors EuTe and EuSe. The established magnetic-dipole mechanism induces bulk SHG polarizations either by the ferromagnetic component of the magnetic structure, or by the spin polarization in the paramagnetic phase. This new type of spin-induced nonlinear susceptibility can appreciably increase the number of centrosymmetric bulk materials, thin films, and artificial structures accessible to nonlinear optics.

This work was supported by the Deutsche Forschungsgemeinschaft (YA65/4-1), the Russian Foundation for Basic Research, Russian Academy Program on Spintronics, FoNE of the European Science Foundation, the Brazilian Agencies FAPESP and CNPq, the Austrian Science Funds (I80-N20) and the FWF (Vienna, Austria).

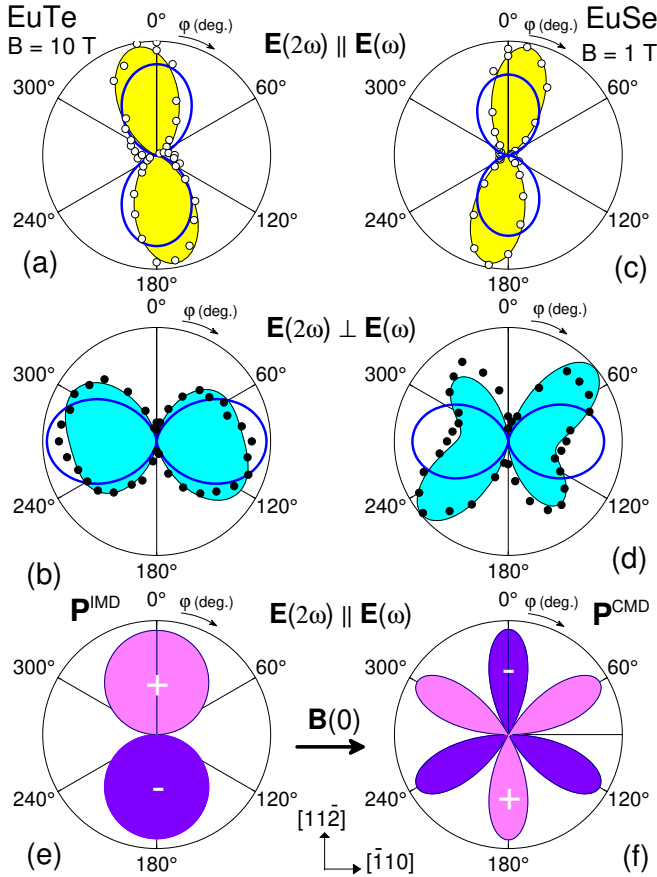


FIG. 3: (Color online) Polar plots of experimental SHG intensity data (dots) in EuTe (a,b) and EuSe (c,d) measured at 2.4 eV. Best fits based on Eqs. (4) and (5), taking into account the IMD (IMD and CMD), are shown by solid lines (shaded areas). Polar plots for calculated IMD (e) and CMD (f) nonlinear polarizations with $m3m$ and $\bar{3}m$ symmetries, respectively.

-
- [1] Y. R. Shen, *The Principles of Nonlinear Optics* (Wiley, New York, 1984).
- [2] R. W. Boyd, *Nonlinear Optics* (Academic, San Diego, 1993).
- [3] M. Fiebig, V. V. Pavlov, and R. V. Pisarev, *J. Opt. Soc. Amer.* **22**, 96 (2005).
- [4] H. P. Wagner *et al.*, *Phys. Phys. B* **58**, 10494 (1998).
- [5] S. Bergfeld and W. Daum, *Phys. Phys. Lett.* **90**, 036801 (2003).
- [6] V. V. Pavlov *et al.*, *Phys. Rev. Lett.* **94**, 157404 (2005).
- [7] I. Sanger *et al.*, *Phys. Rev. Lett.* **96**, 117211 (2006).
- [8] R. W. Terhune, P. D. Maker, and C. M. Savage, *Phys. Rev. Lett.* **8**, 404 (1962).
- [9] P. Wachter, *Handbook on the Physics and Chemistry of Rare Earths*, Vol. 11, Eds. K. A. Gschneider and L. R. Eyring (North Holland, Amsterdam, 1979), p. 507.
- [10] R. T. Lechner *et al.*, *Phys. Phys. Lett.* **94**, 157201 (2005).
- [11] J. Schoenes, and P. Wachter, *IEEE Trans. Magnetics* **MAG12**, 81 (1976).
- [12] A. B. Henriques *et al.*, *Phys. Rev. B* **72**, 155337 (2005).
- [13] A. B. Henriques, M. A. Manfrini, P. H. O. Rappl, and E. Abramof, *Phys. Rev. B* **77**, 035204 (2008).
- [14] G. Springholz *et al.*, *Appl. Phys. Lett.* **79**, 1225 (2001).
- [15] A. Schmehl *et al.*, *Nature. Mat.* **6**, 882 (2007).
- [16] J. Trbovic, C. Ren, P. Xiong, and S. von Molnar, *Appl. Phys. Lett.* **87**, 082101 (2005).
- [17] T. S. Santos *et al.*, *Phys. Rev. Lett.* **101**, 147201 (2008).
- [18] G.-X. Miao, M. Muller, J.S. Moodera, , *Phys. Rev. Lett.* **102**, 076601 (2009).
- [19] W. Heiss, G. Prechtel, and G. Springholz, *Phys. Rev. B* **63**, 165323 (2001).
- [20] N. F. Oliveira, S. Foner, Y. Shapira, and T. B. Reed, *Phys. Rev. B* **5**, 2634 (1972).
- [21] J. E. Sipe, V. Mizrahi, and G. I. Stegeman, *Phys. Rev. B* **35**, 9091 (1987).
- [22] P. S. Pershan, *Phys. Phys.* **130**, 919 (1963).
- [23] R. R. Birss, *Symmetry and Magnetism* (North Holland, Amsterdam, 1967).
- [24] G. F. Koster, J. O. Dimmock, R. G. Wheeler, and H. Schatz, *Properties of the 32 Point Groups* (M.I.T. Press, Cambridge, Massachusetts, USA, 1963).
- [25] G. van der Laan, E. Arenholz, A. Schmehl, and D. G. Schlom, *Phys. Rev. Lett.* **100**, 067403 (2008).
- [26] R. Kirchschlager *et al.*, *Appl. Phys. Lett.* **85**, 67 (2004).